Adaptive Reference Power Based Voltage Droop Control for VSC-MTDC Systems

Yizhen Wang, *Member*, *IEEE*, Fengliang Qiu, Guowei Liu, Ming Lei, Chao Yang, and Chengshan Wang, *Senior Member*, *IEEE*

***Abstract*—Featuring low communication requirements and high reliability, the voltage droop control method is widely adopted in the voltage source converter based multi-terminal direct current (VSC-MTDC) system for autonomous DC voltage regulation and power-sharing. However, the traditional voltage droop control method with fixed droop gain is criticized for over-limit DC voltage deviation in case of large power disturbances, which can threaten stable operation of the entire VSC-MTDC system. To tackle this problem, this paper proposes an adaptive reference power based voltage droop control method, which changes the reference power to compensate the power deviation for droop-controlled voltage source converters (VSCs). Besides retaining the merits of the traditional voltage droop control method, both DC voltage deviation reduction and power distribution improvement can be achieved by utilizing local information and a specific control factor in the proposed method. Basic principles and key features of the proposed method are described. Detailed analyses on the effects of the control factor on DC voltage deviation and imbalanced power-sharing are discussed, and the selection principle of the control factor is proposed. Finally, the effectiveness of the proposed method is validated by the simulations on a five-terminal VSC based high-voltage direct current (VSC-HVDC) system.**

***Index Terms*—DC voltage deviation, power-sharing, reference power, voltage droop control, voltage source converter (VSC), multi-terminal direct current (MTDC).**

I. Introduction

THE utilization of sustainable energy has become an inevitable approach to achieve net-zero carbon emission. Facing the intermittent of renewable energy like wind or solar power, the DC technique provides a promising solution in renewable energy integration [1], [2]. With the decrease of difficulties in manufacturing and expense of semiconductor devices such as insulated gate bipolar transistor (IGBT), more research has been focused on voltage source converters (VSCs) due to their outstanding features. Compared with line commutated converters, the VSC-based high-voltage direct current (VSC-HVDC) technology has advantages such as no commutation failure problem, decoupled active and reactive power control, and capability of power supply to passive systems [3], [4]. Furthermore, the VSC-based multi-terminal direct current (VSC-MTDC) system provides more security redundancy and enhances power exchange flexibility between multiple areas, contributing to less economic losses caused by a potential blackout and lower operating power losses by implementing optimal power flow control [5]. Hence, VSC-MTDC is regarded as an effective solution for integration of large-scale renewable energy like offshore wind energy [6]-[8]. Practical engineering applications such as "Nan'ao ±160 kV three-terminal VSC-HVDC project" and "Zhangbei ±500 kV four-terminal VSC-HVDC project" have demonstrated the benefits of VSC-MTDC systems [9], [10].

To ensure stable operation of the VSC-MTDC system, DC voltage stability must be guaranteed since the DC voltage is regarded as a dominant indicator of power balance in multi-terminal direct current (MTDC) systems [11], [12]. Generally, the existing various control methods regarding DC voltage regulation in MTDC systems can be categorized into two classes: master-slave methods and voltage droop control methods [13]-[15]. The master-slave methods belong to the centralized schemes, which are simple but unreliable due to their demand for fast communication. On the contrary, the voltage droop control methods belong to the distributed scheme, which make each VSC participate in imbalanced power burden sharing and alleviate DC voltage deviation simultaneously by local information without fast communication [14], [16].

Regarding the control framework of VSC-MTDC, the voltage droop control method belongs to the primary control, which commonly employs a proportional controller to maintain system stability during large disturbances as fast as possible [17]. However, the performance of the traditional droop-controlled VSC with fixed droop gain is limited. Since the operation mode of the VSC-MTDC changes under large power disturbances, the DC voltage of the droop-controlled VSC will deviate from the setting value automatically, resulting in hitting the DC voltage safety limit [18]. Meanwhile, improper power redistribution can also emerge in the post-disturbance process. Actually, how to maintain

Manuscript received: May 19, 2021; revised: July 25, 2021; accepted: September 7, 2021. Date of CrossCheck: September 7, 2021. Date of online publication: October 29, 2021.

This work was supported by the Key Science and Technology Projects of China Southern Power Grid Corporation (No. 090000KK52180116) and National Natural Science Foundation of China (No. 51807135).

Y. Wang, F. Qiu, M. Lei (corresponding author), and C. Wang are with Key Laboratory of Smart Grid of Ministry of Education, Key Laboratory of Smart Energy & Information Technology of Tianjin Municipality, Tianjin 300072, China (e-mail: yizhen.wang@tju.edu.cn; 13786306050@163.com; ming.lei@tju.edu.cn; cswang@tju.edu.cn).

G. Liu is with Shenzhen Power Supply Bureau Co., Ltd., Shenzhen 518001, China (e-mail: liulgw@yeah.net).

C. Yang is with Sichuan Energy Internet Research Institution, Tsinghua University, Chengdu 610213, China (e-mail: chaoyang@tsinghua-eiri.org).

DOI: 10.35833/MPCE.2021.000307

DC voltage of VSC-MTDC system within specified range during large disturbances is a critical issue and has drawn intensive attention from both academy and industry.

To cope with the limitations of the traditional fixed droop gain based voltage droop control method, many methods have been proposed in the literature. Basically, most of the existing studies focus on the adaptive voltage droop control method, which adaptively changes the droop gains (coefficients) of the droop-controlled VSCs [19]. Considering the local information including DC voltage and power-sharing factors, [20] changes the droop gains to guarantee the DC voltage deviation and loading rate of each droop-controlled converter below its safety limits. In [21], the droop gain is regulated according to a function of the normalized available power headroom of each droop-controlled converter. In [22], the droop gain of the droop-controlled VSC is set to improve stability margin, but the transient performance is not considered. Based on the distributed consensus algorithm, frequency support is achieved in [23] via adaptive droop gain. By decreasing the total incremental generation cost, the adaptive droop gain in [24] is tuned to improve the economic operation of the MTDC system. Nevertheless, the variation of the droop gain not only affects the system operation, but also leads to instability of the MTDC system [25]. In addition, [26] develops a comprehensive approach to determine the droop gains, which are divided into two parts according to the over-voltage and under-voltage containment reserves. Likewise, [27] changes the setpoints according to the calculation from the improved AC-DC power flow algorithm to minimize the DC voltage deviation and transmission losses at the same time. These control schemes, however, impose requirements on communication and change the relevant parameters only when the instruction signal is received.

Motivated by the aforementioned problems, this paper proposes an adaptive reference power based voltage droop control method for VSC-MTDC systems. The main contributions of this paper are as follows.

1) Without tuning the droop gain, the local power deviation is utilized to compensate the original reference power, which achieves the movement of the DC voltage to its nominal value and reduction of the DC voltage over-limit risk.

2) A control factor is introduced into the proposed method to indicate the degree of compensation for the original reference power, which also realizes different *P-V* characteristics in different VSCs. The influences of the control factor on DC voltage deviation and imbalanced power-sharing are discussed, and the selection principle of the control factor is proposed.

3) Besides retaining the high reliability of the traditional voltage droop control method, the proposed method continuously adjusts the reference power for restricting the DC voltage deviation and improving the power distribution in the post-disturbance process.

The remainder of this paper is organized as follows. The control structure of a VSC station and the working principle on the traditional voltage droop control method are introduced in Section II. The adaptive reference power based voltage droop control method and the discussion of the control factor are presented in Section III. In Section IV, the simulations on a five-terminal VSC-HVDC system are conducted in PSCAD/EMTDC to validate the effectiveness of the proposed method. Finally, conclusions are presented in Section V.

II. Control Structure of VSC Station and Working Principle of Traditional Voltage Droop Control Method

The intrinsic characteristics of the traditional voltage droop control method are the theoretical foundation of the proposed method. Therefore, the control structure of a VSC station and the working principle of traditional voltage droop control method are described first. For simplicity, this paper adopts the per-unit system and assumes that the direction of the power injected into the DC system is positive.

A. Control Structure of a VSC Station

The schematic diagram of a VSC station is shown in Fig. 1, where the AC bus is the point of common coupling (PCC). The corresponding control structure including block diagrams of the voltage droop control and the decoupled current control is illustrated in Fig. 2. Usually, the typical control structure of a VSC station consists of the inner current control loop and the outer control loop [22]. The inner current control loop regulates the measured current according to its reference generated by the outer control loop, which operates with the constant active power, constant DC voltage, and voltage droop control. The dynamic equations of the VSC current can be given as:

$$\begin{cases} L_{\mathrm{eq}}\dfrac{\mathrm{d}i_d}{\mathrm{d}t} = -R_{\mathrm{eq}}i_d - \omega_{\mathrm{g}}L_{\mathrm{eq}}i_q - v_{d,\mathrm{ref}} + v_d \\ L_{\mathrm{eq}}\dfrac{\mathrm{d}i_q}{\mathrm{d}t} = -R_{\mathrm{eq}}i_q + \omega_{\mathrm{g}}L_{\mathrm{eq}}i_d - v_{q,\mathrm{ref}} + v_q \end{cases} \tag{1}$$

where R_{eq}, L_{eq}, and C_{eq} are the equivalent resistance, inductance, and capacitance of the VSC, respectively; i_d and i_q are the d and q components of the current flowing from the AC system to the converter side, respectively; ω_{g} is the angular frequency of the AC system; $v_{d,\mathrm{ref}}$ and $v_{q,\mathrm{ref}}$ are the d and q components of the reference output AC voltage of VSC, respectively; and v_d and v_q are the d and q components of the AC voltage at PCC, respectively.

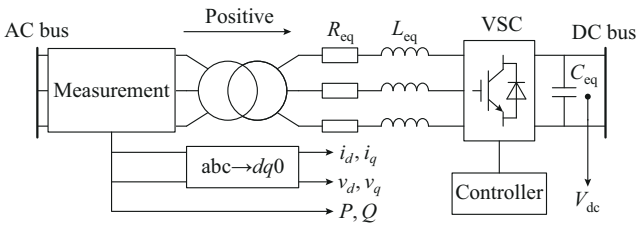

Fig. 1. Schematic diagram of a VSC station.

The reactive power control class contains the constant reacitve power control and constant AC voltage control. The active power control class contains the constant active power, constant DC voltage, and voltage droop control. Particularly, both constant voltage control and constant power control can be regarded as extreme cases of the voltage droop control method. In other words, the voltage droop control method is a tradeoff between them.

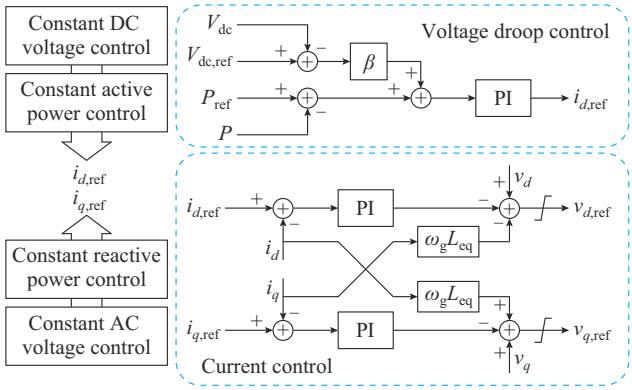

Fig. 2. Control structure of a VSC station.

B. Working Principle of Traditional Voltage Droop Control Method

As depicted in Fig. 3, the relationship of the DC voltage and the exchanged power in the voltage droop control method can be expressed as:

$$(P-P_{\text{ref}})+\beta(V_{\text{dc}}-V_{\text{dc,ref}})=0 \tag{2}$$

where P_{ref} and P are the reference and the measured exchanged active power injected into the DC side from the AC system, respectively; $V_{\text{dc,ref}}$ and V_{dc} are the reference and measured DC voltages, respectively; and β is the droop gain, which is defined as the ratio of the change in active power to the change in DC voltage.

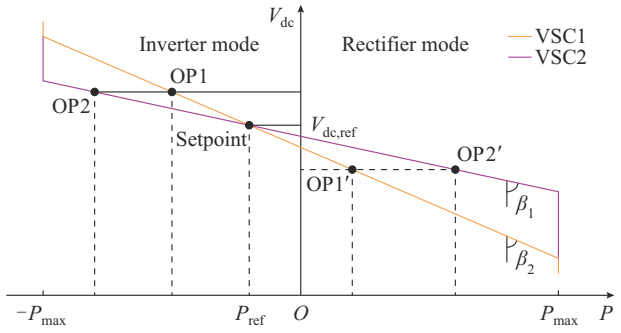

Fig. 3. *P-V* characteristic curves of traditional voltage droop control method.

Given that the VSC-MTDC system is an ideal lossless grid, two VSCs (VSC1 and VSC2) adopt the traditional voltage droop control method and no other converters participate in DC voltage control. Since there are no power losses in this VSC-MTDC system, the DC voltages of the two VSCs are identical. As shown in Fig. 3, when some disturbances occur, the operating points (OP1 and OP2) of the two VSCs will move along with their *P-V* characteristic curves and reach the new operating points (OP1′ and OP2′), resulting in DC voltages deviating from their original operating points. The two VSCs will share the imbalanced power by:

$$\Delta P=\sum_{i=1}^{2}\Delta P_i=-\sum_{i=1}^{2}\beta_i\Delta V_{\text{dc}i}=-(\beta_1+\beta_2)\Delta V_{\text{dc}} \tag{3}$$

where ΔP is the imbalanced power; ΔP_i is the imbalanced power shared by VSCi; $\Delta V_{\text{dc}i}$ is the DC voltage deviation between the operating points before and after disturbances of the VSCi and all the $\Delta V_{\text{dc}i}$ are equal to ΔV_{dc}; and β_1 and β_2 are the droop gains of VSC1 and VSC2, respectively. Thus, the shared imbalanced power of each VSC is:

$$\Delta P_i=-\beta_i\Delta V_{\text{dc}i}=\frac{-\beta_i\Delta V_{\text{dc}i}}{-(\beta_1+\beta_2)\Delta V_{\text{dc}}}\Delta P=\frac{\beta_i}{\beta_1+\beta_2}\Delta P \quad i=1,2 \tag{4}$$

According to (4), in an ideal lossless grid, the imbalanced power is shared by droop-controlled converters in proportion to their droop gains. Consequently, the dispatcher can design the droop gain according to the power-sharing with post-disturbance. However, when considering the resistance of the transmission line, DC line voltage drops in the VSC-MTDC system will cause non-uniform variation of the DC bus voltage, which in turn affects the imbalanced power redistribution among droop-controlled converters [28].

III. Adaptive Reference Power Based Voltage Droop Control Method

A. Adaptive Reference Power

When adopting the voltage droop control method with fixed droop gain (denoted as fixed method), the gap between the measured DC voltage and the reference DC voltage should be smaller when the measured power gets close to the reference power. Therefore, the direct approach to reducing the DC voltage deviation is to adjust the reference power of the setpoint. Furthermore, the adjustment of the reference power can be described as a movement of the *P-V* droop characteristic curve of the voltage droop control method on the *P-V* plane. Based on these analyses, changing the reference power adaptively should be an effective approach to achieve the improvement of the VSC-MTDC system with large disturbances.

As illustrated in Fig. 4, the imbalanced power leads to DC voltage deviation, where F1, A1, and B1 are the setpoints; F2, A2, and B2 are the operating points; and C12 is the setpoint as well as operating point. To be more intuitive, the imbalanced power in Fig. 4 is assumed to be a constant. Considering that the reference power can be compensated based on the difference between the measured power and the reference power, the DC voltage deviation will be significantly reduced. For example, since Line B has more compensation power than Line A, Line A operates at a point with a larger DC voltage deviation. Hence, the adaptive reference power can be expressed as:

$$P_{\text{ref,new}}=P_{\text{ref0}}+K\Delta P_{\text{de}} \tag{5}$$

where $P_{\text{ref,new}}$ is the new reference power; P_{ref0} is the initial-setting reference power; K is the compensation factor; and ΔP_{de} is the power deviation, which is defined as:

$$\Delta P_{\text{de}}=P-P_{\text{ref0}} \tag{6}$$

In accordance with the characteristic of the traditional voltage droop control method, the larger DC voltage deviation is, the more imbalanced power needs to be compensated to limit the DC voltage deviation. Therefore, the novel expression of the compensation factor proposed in this paper can be represented as:

$$K=\frac{1}{\dfrac{\alpha}{|\delta|}+|P_{\text{ref0}}|} \tag{7}$$

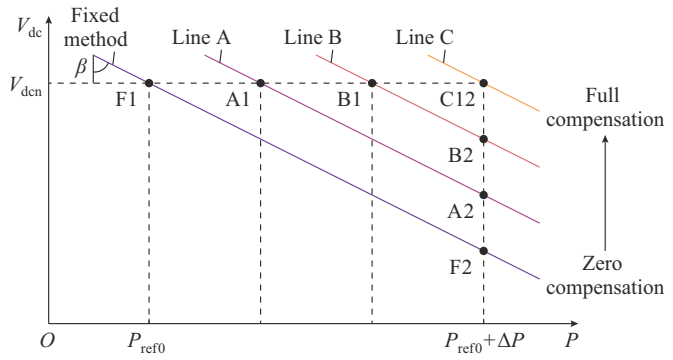

Fig. 4. *P-V* characteristics, setpoints, and operating points of proposed method with different compensation factors.

where α is the control factor, which is an important constant that determines the compensation degree and is discussed in detail in Section III-C and D; and δ is the DC voltage deviation, which can be expressed as:

$$\delta = V_{dc} - V_{dcn} \tag{8}$$

where V_{dcn} is the nominal DC voltage. Combing (5), (6), and (7), the adaptive reference power can be expressed as:

$$P_{ref,new} = P_{ref0} + \frac{P - P_{ref0}}{\frac{\alpha}{|\delta|} + |P_{ref0}|} \tag{9}$$

Equation (9) indicates that a larger DC voltage deviation causes a larger compensation factor. Moreover, if $\delta \to 0$, then $K \to 0$, which means that the reference power will not be compensated if the DC voltage deviation is negligible. Besides, the initial-setting reference power in (7) and (9) contributes to the improvement of power distribution under post-disturbance. As explained in Fig. 5, the converter with a smaller initial-setting reference power will share more imbalanced power in the VSC-MTDC system, where A_1 and B_1 are the initial setpoints; C_1 and D_1 are the new setpoints generated by the proposed method; A_2 and B_2 are the operating points generated by the fixed method after disturbance; and C_2 and D_2 are the operating points generated by the proposed method after disturbance.

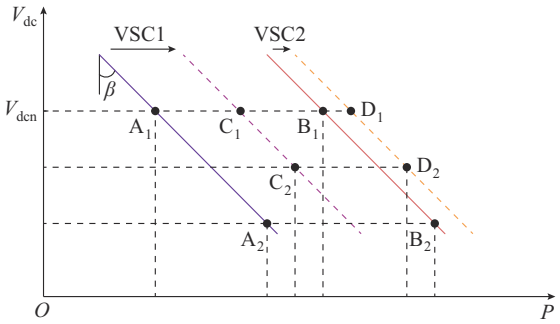

Fig. 5. *P-V* characteristics, setpoints, and operating points of proposed method and fixed method.

Taking (2), (8), and (9) into consideration, the block diagram of the proposed method is depicted in Fig. 6, where N denotes the numerator, and D denotes the denominator.

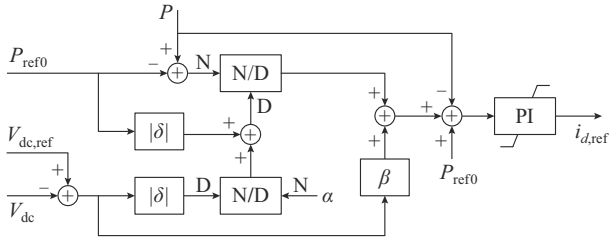

Fig. 6. Block diagram of proposed method.

B. Basic Features of Proposed Method

According to (8) and (9), the basic features of the proposed method are described as follows.

1) When a droop-controlled VSC works at the rectifier mode, the DC voltage will decrease as the rectifier power increases. After adopting the proposed method, the reference power P_{ref} will increase when the measured power P is greater than the initial-setting value P_{ref0}, which means the *P-V* characteristic curve rises for compensating for the DC voltage drop.

2) When a droop-controlled VSC works in the inverter mode, the DC voltage will increase as the inverter power increases. After adopting the proposed method, the reference power P_{ref} will decrease when the measured power P is smaller than the initial-setting value P_{ref0}, which means the *P-V* characteristic curve drops for compensating for the DC voltage rising.

3) When the absolute value of DC voltage deviation $|\delta|$ is small enough, the value of the denominator in (9) will be big enough. Therefore, the adjustment value of the reference power will also be small, and vice versa.

4) Assuming the control factors and DC voltage deviations of different VSCs are identical, the VSC with a higher power loading rate will share less imbalanced power.

5) The control factor α determines the compensation degree of the original reference power. In general, the control factor α is related to the DC voltage deviation and initial-setting reference power. Moreover, different VSCs can regulate their control factors independently to achieve better performance.

In summary, the proposed method can enhance the ability of converters to sustain the DC voltage.

C. Ranges of Control Factor

The control factor α in (9) plays a significant role in the proposed method. Therefore, the range of the control factor α should be discussed in detail.

First of all, the steady-state power of VSC is calculated. Since the input of the proportional-integral (PI) regulator in Fig. 6 must be zero in steady state, the exchanged power of a VSC in steady state can be calculated as:

$$P = P_{ref0} - \frac{\beta\delta\left(\frac{\alpha}{|\delta|} + |P_{ref0}|\right)}{\frac{\alpha}{|\delta|} + |P_{ref0}| - 1} \tag{10}$$

Apparently, $|P_{ref0}| \le 1$. Besides, one of the most important requirements of the voltage droop control method is to ensure the derivative of the exchanged power to DC voltage deviation is monotonous (negative in this paper). Otherwise, it is impossible for the MTDC system to achieve a new

steady state mathematically, which indicates that:

$$\frac{\partial P}{\partial \delta} < 0 \tag{11}$$

Considering the adjustment margin in (5) and avoiding the instability caused by the excessive adjustment, the range of the compensation factor K in (5) should be 0 to 1. Thus, it is reasonable to assume $\alpha/|\delta| + |P_{\text{ref0}}| > 1$ in (10).

If $\delta > 0$, substituting (10) into (11) yields:

$$\alpha > \delta\left(\sqrt{|P_{\text{ref0}}|} - |P_{\text{ref0}}|\right) \tag{12}$$

If $\delta < 0$, substituting (10) into (11) yields:

$$\alpha > -\delta\left(\sqrt{|P_{\text{ref0}}|} - |P_{\text{ref0}}|\right) \tag{13}$$

Therefore, the range of control factor is:

$$\alpha > |\delta|\left(\sqrt{|P_{\text{ref0}}|} - |P_{\text{ref0}}|\right) \tag{14}$$

As a conservative condition, it is assumed that $\alpha > |\delta|\left(1 - |P_{\text{ref0}}|\right)$. For simplicity and convenience, it is further assumed that $|\delta|$ is set as the limit of the DC voltage deviation $\delta_{\max}$. Therefore, the lower limit of the control factor can be simplified as:

$$\alpha > \delta_{\max}\left(1 - |P_{\text{ref0}}|\right) \tag{15}$$

where $\delta_{\max}$ is usually ranged between 5% and 10%.

Moreover, some other conditions should also be satisfied to maintain stable operation of the VSC-MTDC system. For example, the power loading rate of the droop-controlled VSC should be 1 when the DC voltage deviation hits its limit $\delta_{\max}$. Therefore, the control factor α should meet the following requirement.

$$\alpha < \delta_{\max}\left(\frac{S + |P_{\text{ref0}}|}{S + |P_{\text{ref0}}| - \beta\delta_{\max}} - |P_{\text{ref0}}|\right) \tag{16}$$

where S is the nominal capacity of the VSC.

Whereas, (16) is established in the case that the VSC station operates in both inverter and rectifier modes. The range of the control factor is excessive for the VSC that only operates in inverter or rectifier mode. Hence, for the droop-controlled inverter station, the following conditions should be satisfied.

1) When the DC voltage deviation is $\delta_{\max}$, the exchanged power of the droop-controlled inverter station is −1.

2) When the DC voltage deviation is $-\delta_{\max}$, the exchanged power of the droop-controlled inverter station is 0.

Thus, the requirement of control factor α is expressed as:

$$\alpha < \delta_{\max}\left(\frac{S + P_{\text{ref0}}}{S + P_{\text{ref0}} - \beta\delta_{\max}} + P_{\text{ref0}}\right) \tag{17}$$

Similarly, the requirement of control factor α for the droop-controlled rectifier is expressed as:

$$\alpha < \delta_{\max}\left(\frac{S - P_{\text{ref0}}}{S - P_{\text{ref0}} - \beta\delta_{\max}} - P_{\text{ref0}}\right) \tag{18}$$

It should be noted that the premise of (16) is:

$$S + |P_{\text{ref0}}| - \beta\delta_{\max} > 0 \tag{19}$$

Furthermore, the premise of (17) and (18) is:

$$S - |P_{\text{ref0}}| - \beta\delta_{\max} > 0 \tag{20}$$

When (19) and (20) are not satisfied, the upper limit of the control factor is positive infinity.

In summary, the ranges of the control factor α should satisfy (15) and the requirements of loading ratios simultaneously. The exact value of the control factor can be chosen flexibly based on the above discussion. It can be tuned according to the converter capacity and the actual grid topology.

D. Influence of Control Factor

According to (11), if $\alpha \to \infty$, then $P \to P_{\text{ref0}} - \beta\delta$, which means that the proposed method degenerates to the fixed method. In this part, a simple case is studied to demonstrate the influence of the control factor α on the proposed method. The basic parameters of this simple case are listed in Table I.

TABLE I
BASIC PARAMETERS OF SIMPLE CASE

Description	Value (p.u.)
Initial-setting reference power	−0.3
Reference DC voltage	1
Droop gain	10
Limit of voltage deviation	0.05

Assuming that the VSC station only operates in the inverter mode and taking the parameters listed in Table I into (15) and (17), the range of the control factor is obtained, which is $0.035 < \alpha < 0.16$. The *P-V* characteristic curves of the proposed method with different control factors are shown in Fig. 7(a). The curves with recommended control factors are between the two curves with $\alpha = 0.16$ and $\alpha = 0.035$. Actually, the *P-V* characteristic described in this paper is achieved by adjusting the setpoints of the voltage droop control method, which is different from the conventional method by directly tuning the *P-V* characteristic curves [29]. As observed in Fig. 7(a), the *P-V* characteristic curve is more bent with a smaller control factor.

The influence of the control factor α on exchanged power with identical DC voltage deviation is illustrated in Fig. 7(b). It shows that the VSC will share more imbalanced power as the control factor decreases and the absolute value of the DC voltage deviation increases. It is worth mentioning that points (−1.0 p.u., 0.06625) and (1.0 p.u., 0.16) highlighted in Fig. 7(b) are consistent with the results calculated from (16) and (17).

IV. SIMULATION VERIFICATION

To validate the proposed method, simulations of a ±200 kV five-terminal VSC-HVDC system are investigated using PSCAD/EMTDC. As shown in Fig. 8, the five-terminal VSC-HVDC system delivers the wind power from VSC4 and VSC5 to the other three strong and separate AC systems through VSC1, VSC2, and VSC3. During normal operation, both VSC4 and VSC5 are in the mode of regulating the AC voltage and the frequency of their PCCs. VSC1, VSC2, and VSC3 adopt the voltage droop control method, and the output reactive power of them is zero. The main parameters of this VSC-MTDC system are listed in Table II.

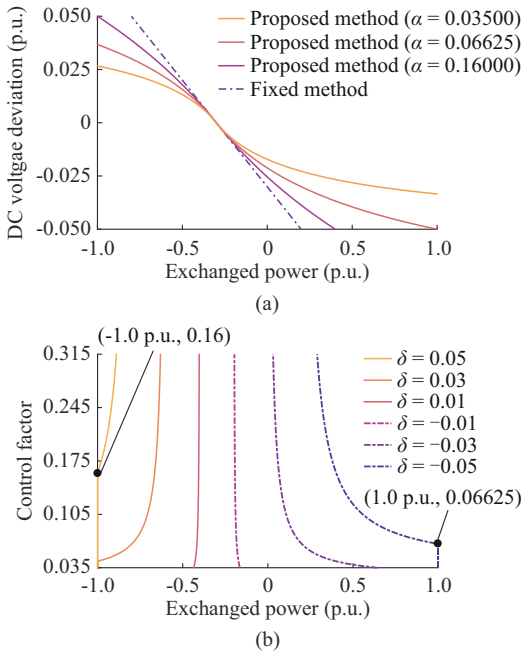

Fig. 7. *P-V* characteristic curves of proposed method with different control factors. (a) *P-V* characteristic curves at a given setpoint. (b) Influence of control factors on exchanged power.

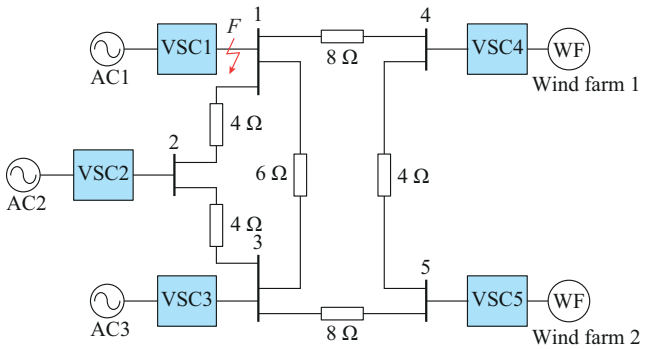

Fig. 8. Diagram of a five-terminal VSC-HVDC system.

As discussed in the previous section, smaller control factors result in VSCs sharing more imbalanced power in case of power disturbances. Consequently, considering the capacity of each VSC station, the control factor of VSC1 should be large and the control factor of VSC2 should be small. According to (15), (17), and the parameters in Table II, VSC1, VSC2, and VSC3 have the same range of the control factor, which is between 0.035 and 0.16. In this case, $\alpha_1 = 0.15$, $\alpha_2 = 0.04$, and $\alpha_3 = 0.08$ are selected.

The large power fluctuation of renewable energy and the VSC station outage are common disturbances to the VSC-MTDC system.

Since this paper focuses on the regulation performance of DC voltage and exchanged power, the complicated fault process is omitted and the ideal DC circuit breaker that can isolate DC faults immediately is assumed. Therefore, the power step and VSC station outage are selected as the disturbances in this case and the detailed description is presented as follows.

1) Disturbance F1: at 2.2 s, the output power of wind farm 1 steps from 200 MW to 500 MW, and the output power of wind farm 2 steps from 260 MW to 460 MW.

TABLE II
PARAMETERS OF VSC-MTDC SYSTEM

Description	Value
Nominal capacity of VSC1	200 MVA
Nominal capacity of VSC2	600 MVA
Nominal capacity of VSC3	400 MVA
Nominal capacity of VSC4	600 MVA
Nominal capacity of VSC5	600 MVA
Initial-setting reference power of VSC1	−60 MW
Initial-setting reference power of VSC2	−180 MW
Initial-setting reference power of VSC3	−120 MW
Droop gain of VSC1, VSC2, and VSC3	10 p.u.
Limit of voltage deviation (δ_{max})	5%
Control factor of VSC1 (α_1)	0.15
Control factor of VSC2 (α_2)	0.04
Control factor of VSC3 (α_3)	0.08
Valve-side AC voltage	230 kV
Nominal DC voltage	±200 kV
Proportional gain of outer-loop PI controller	2
Integral time constant of outer-loop PI controller	0.1 s
Proportional gain of inner-loop PI controller	0.6
Integral time constant of inner-loop PI controller	0.01 s

2) Disturbance F2: at 3.2 s, VSC1 is disconnected from the system, which is depicted at *F* in Fig. 8.

The comparison between the fixed method and the proposed method is studied. The simulation results of DC voltage and exchanged power of the droop-controlled VSCs during the above two disturbances are illustrated in Fig. 9 and Fig. 10, respectively. In Fig. 9, V_{dci} is the DC voltage of the VSC*i*. In Fig. 10, P_i is the exchanged power of the VSC*i*. Furthermore, the simulation results of exchanged power of VSC4 and VSC5 are also presented in Fig. 10. As can be observed, the measured power under these two methods is the same and both curves almost coincide. Meanwhile, the power loading ratios of droop-controlled VSCs before and after F1 and F2 are listed in Table III to investigate the impact of control factor α.

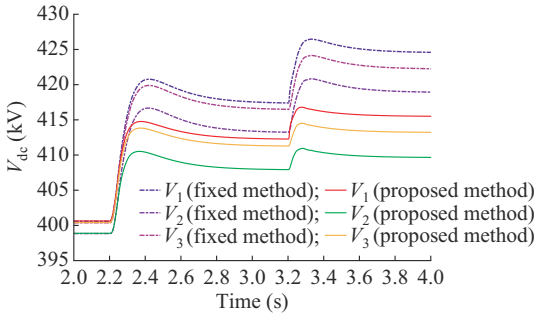

Fig. 9. Simulations of DC voltage with proposed method and fixed method.

The DC voltages and exchanged power of all VSCs with these two methods are almost the same before 2.2 s. It indicates that the proposed method has a similar performance with the fixed method in the case of a small absolute value of DC voltage deviation.

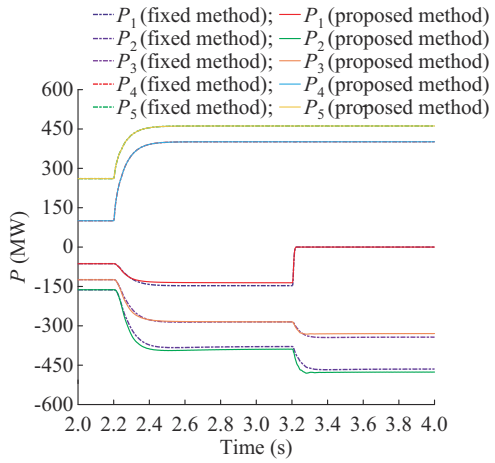

Fig. 10. Simulations of exchanged power with proposed method and fixed method.

TABLE III
LOADING RATIOS OF DROOP-CONTROLLED VSCS BEFORE AND AFTER DISTURBANCES F1 AND F2

Situation	Method	Loading ratio (%)		
		VSC1	VSC2	VSC3
Before F1	Proposed	31.68	27.08	31.12
	Fixed	31.57	27.18	31.02
After F1 and before F2	Proposed	67.92	64.83	71.23
	Fixed	73.48	63.17	71.25
After F2	Proposed	0.00	79.38	82.39
	Fixed	0.00	77.46	85.78

When F1 occurs, the output power of the windfarms steps from 460 MW to 960 MW, which raises the total power injected into the VSC-MTDC system. As the DC voltage rises, the droop-controlled VSCs start compensating for the imbalanced power after F1.

The DC voltage of VSC1 with fixed method exceeds the safety limit during the dynamic process. On the contrary, the DC voltages of droop-controlled VSCs with the proposed method are within the specified range and have lower DC voltage deviations compared with those of the VSCs adopting the fixed method.

The results in Table III and Fig. 10 demonstrate that VSC2 with a smaller control factor has a larger compensation factor and undertakes more imbalanced power. Compared with the fixed method, the proposed method increases the exchanged power of VSC2 and decreases that of VSC1. Therefore, these results are in accordance with the conclusion in Section III-D and confirm the influence of control factor on exchanged power.

At 3.2 s, VSC1 outage occurs and the DC circuit breaker activates quickly. After F2, the exchanged power of VSC1 decreases to zero, which indicates the reduction in power absorbed from the entire VSC-MTDC system. Consequently, the positive power mismatch causes the increase of DC voltage.

As shown in Fig. 9, the DC voltages of the droop-controlled VSCs with fixed method exceed the safety limit again, and the maximum value reaches 426 kV. Moreover, the DC voltages of VSC1 and VSC3 at steady state are still higher than 420 kV. Compared with the fixed method, the proposed method can ensure the DC voltage deviation below the limit of 420 kV. Besides, the DC voltage deviation of each VSC with the proposed method is smaller than that with the fixed method. As depicted in Fig. 10, the fast response of VSC2 compensates for the imbalanced power quickly and restricts the increase of DC voltage. The results in Table III once again demonstrate that VSC3 reduces its loading ratio due to a larger control factor.

Figure 11 shows the reference power of droop-controlled VSCs with the proposed method. When the output power of wind farms increases, the reference power of droop-controlled VSCs decreases. When VSC1 disconnects from the VSC-MTDC system, the reference power of VSC2 and VSC3 also decreases. The compensation degree of original reference power of VSC2 is greater than that of VSC3, while VSC1 has the least compensation degree value. Despite that the DC voltage deviation of VSC2 is the lowest, VSC2 shares the most imbalanced power due to its smaller control factor and larger compensation factor. The results illustrated in Fig. 11 are consistent with those in Fig. 9, Fig. 10, and the results discussed in Section III.

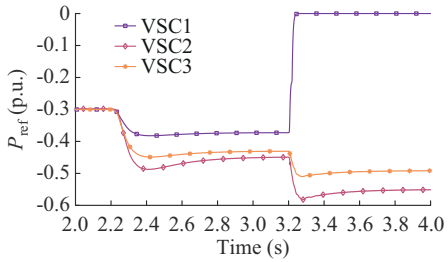

Fig. 11. Simulations of reference power of droop-controlled VSCs with proposed method.

In summary, compared with the fixed method, the proposed method maintains the DC voltages of droop-controlled VSCs within their safety limits during large power variation and VSC outage. Besides, it alleviates the improper distribution of the imbalanced power.

V. CONCLUSION

In the light of the inherent characteristics of the traditional voltage droop control, the adaptive reference power based voltage droop control method is proposed. The proposed method revises the reference power to compensate the power deviation for the droop-controlled VSC to reduce the DC deviation of the VSC-MTDC system. The compensation degree is determined by the control factor, DC voltage deviation, and initial-setting reference power. Based on *P-V* characteristic curves, the intrinsic principle and basic features of the proposed method are described. Furthermore, the selection principle of the control factors is studied and detailed analyses regarding the effects of the control factor on DC voltage deviation and exchanged power are discussed. Besides retaining the high reliability of the traditional voltage droop control method, the proposed method restricts the DC voltage of droop-controlled VSCs within the safety limit and adjusts

the DC voltage to its rated value. Moreover, the proposed method rationalizes the imbalanced power redistribution and realizes the diversity of power-sharing among VSCs in post-disturbance process by setting different control factors. Finally, a case study of a five-terminal VSC-HVDC system integrated with two wind farms validates the effectiveness of the proposed method. Future studies will focus on the integration of optimal dispatch with the proposed method for VSC-MTDC systems.

REFERENCES

[1] N. R. Watson and J. D. Watson, "An overview of HVDC technology," *Energies*, vol. 13, no. 17, p. 4342, Aug. 2020.

[2] B. Yang, L. Jiang, T. Yu *et al*., "Passive control design for multi-terminal VSC-HVDC systems via energy shaping," *International Journal of Electrical Power & Energy Systems*, vol. 98, pp. 496-508, Jun. 2018.

[3] Y. Zhang, J. Ravishankar, J. Fletcher *et al*., "Review of modular multilevel converter based multi-terminal HVDC systems for offshore wind power transmission," *Renewable and Sustainable Energy Reviews*, vol. 61, pp. 572-586, Aug. 2016.

[4] E. Karami, G. B. Gharehpetian, H. Mohammadpour *et al*., "Generalised representation of multi-terminal VSC-HVDC systems for AC-DC power flow studies," *IET Energy Systems Integration*, vol. 2, no. 1, pp. 50-58, Mar. 2020.

[5] B. Li, Q. Li, Y. Wang *et al*., "A novel method to determine droop coefficients of DC voltage control for VSC-MTDC system," *IEEE Transactions on Power Delivery*, vol. 35, no. 5, pp. 2196-2211, Oct. 2020.

[6] S. Khan and S. Bhowmick, "A generalized power-flow model of VSC-based hybrid AC-DC systems integrated with offshore wind farms," *IEEE Transactions on Sustainable Energy*, vol. 10, no. 4, pp. 1775-1783, Oct. 2019.

[7] Z. Yuan, Y. Wang, Y. Yi *et al*., "Fast linear power flow algorithm for the study of steady-state performance of DC grid," *IEEE Transactions on Power Systems*, vol. 34, no. 6, pp. 4240-4248, Nov. 2019.

[8] J. A. Ansari, C. Liu, and S. A. Khan, "MMC based MTDC grids: a detailed review on issues and challenges for operation, control and protection schemes," *IEEE Access*, vol. 8, pp. 168154-168165, Jun. 2020.

[9] H. Rao, "Architecture of Nan'ao multi-terminal VSC-HVDC system and its multi-functional control," *CSEE Journal of Power and Energy Systems*, vol. 1, no. 1, pp. 9-18, Mar. 2015.

[10] H. Pang and X. Wei, "Research on key technology and equipment for Zhangbei 500 kV DC grid," in *Proceedings of 2018 International Power Electronics Conference*, Niigata, Japan, May 2018, pp. 2343-2351.

[11] Z. Liu and X. Guo, "Control strategy optimization of voltage source converter connected to various types of AC systems," *Journal of Modern Power Systems and Clean Energy*, vol. 9, no. 1, pp. 77-84, Jan. 2021.

[12] K. Sun, H. Xiao, J. Pan *et al*., "Cross-seam hybrid MTDC system for integration and delivery of large-scale renewable energy," *Journal of Modern Power Systems and Clean Energy*, vol. 9, no. 6, pp. 1352-1362, Nov. 2021.

[13] T. K. Vrana, J. Beerten, R. Belmans *et al*., "A classification of DC node voltage control methods for HVDC grids," *Electric Power Systems Research*, vol. 103, pp. 137-144, Oct. 2013.

[14] J. Beerten, S. Cole, and R. Belmans, "Modeling of multi-terminal VSC HVDC systems with distributed DC voltage control," *IEEE Transactions on Power Systems*, vol. 29, no. 1, pp. 34-42, Jan. 2014.

[15] Z. Wang, J. He, Y. Xu *et al*., "Distributed control of VSC-MTDC systems considering tradeoff between voltage regulation and power sharing," *IEEE Transactions on Power Systems*, vol. 35, no. 3, pp. 1812-1821, May 2020.

[16] H. Li, C. Liu, G. Li *et al*., "An enhanced DC voltage droop-control for the VSC-HVDC grid," *IEEE Transactions on Power Systems*, vol. 32, no. 2, pp. 1520-1527, Mar. 2017.

[17] R. H. Renner and D. van Hertem, "Potential of using DC voltage restoration reserve for HVDC grids," *Electric Power Systems Research*, vol. 134, pp. 167-175, May 2016.

[18] Y. Wang, B. Li, Z. Zhou *et al*., "DC voltage deviation-dependent voltage droop control method for VSC-MTDC systems under large disturbances," *IET Renewable Power Generation*, vol. 14, no. 5, pp. 891-896, Mar. 2020.

[19] X. Chen, L. Wang, H. Sun *et al*., "Fuzzy logic based adaptive droop control in multiterminal HVDC for wind power integration," *IEEE Transactions on Energy Conversion*, vol. 32, no. 3, pp. 1200-1208, Sept. 2017.

[20] Y. Wang, W. Wen, C. Wang *et al*., "Adaptive voltage droop method of multiterminal VSC-HVDC systems for DC voltage deviation and power sharing," *IEEE Transactions on Power Delivery*, vol. 34, no. 1, pp. 169-176, Feb. 2019.

[21] N. R. Chaudhuri and B. Chaudhuri, "Adaptive droop control for effective power sharing in multi-terminal DC (MTDC) grids," *IEEE Transactions on Power Systems*, vol. 28, no. 1, pp. 21-29, Feb. 2013.

[22] A. Moawwad, E. F. El-Saadany, and M. S. E. Moursi, "Dynamic security-constrained automatic generation control (AGC) of integrated AC/DC power networks," *IEEE Transactions on Power Systems*, vol. 33, no. 4, pp. 3875-3885, Jul. 2018.

[23] M. N. Ambia, K. Meng, W. Xiao *et al*., "Adaptive droop control of multi-terminal HVDC network for frequency regulation and power sharing," *IEEE Transactions on Power Systems*, vol. 36, no. 1, pp. 566-578, Jan. 2021.

[24] S. Song, R. A. McCann, and G. Jang, "Cost-based adaptive droop control strategy for VSC-MTDC system," *IEEE Transactions on Power Systems*, vol. 36, no. 1, pp. 659-669, Jan. 2021.

[25] R. Wang, Q. Sun, W. Hu *et al*., "Stability-oriented droop coefficients region identification for inverters within weak grid: an impedance-based approach," *IEEE Transactions on Systems, Man, and Cybernetics: Systems*, vol. 51, no. 4, pp. 2258-2268, Apr. 2021.

[26] K. Shinoda, A. Benchaib, J. Dai *et al*., "Over- and under-voltage containment reserves for droop-based primary voltage control of MTDC grids," *IEEE Transactions on Power Delivery*. doi: 10.1109/TPWRD.2021.3054183

[27] Y. Zhang, X. Meng, A. M. Shotorbani *et al*., "Minimization of AC-DC grid transmission loss and DC voltage deviation using adaptive droop control and improved AC-DC power flow algorithm," *IEEE Transactions on Power Systems*, vol. 36, no. 1, pp. 744-756, Jan. 2021.

[28] T. M. Haileselassie and K. Uhlen, "Impact of DC line voltage drops on power flow of MTDC using droop control," *IEEE Transactions on Power Systems*, vol. 27, no. 3, pp. 1441-1449, Aug. 2012.

[29] A. Marten, F. Sass, and D. Westermann, "Continuous *P-V*-characteristic parameterization for multi-terminal HVDC systems," *IEEE Transactions on Power Delivery*, vol. 32, no. 4, pp. 1665-1673, Aug. 2017.

Yizhen Wang is an Associate Professor with the School of Electrical Engineering and Automation, Tianjin University, Tianjin, China. His current research interests include power system stability analysis, power system protection, and VSC-HVDC systems.

Fengliang Qiu received the B.S. degree in electrical engineering from Tianjin University, Tianjin, China, in 2020. He is currently working toward the M.E.E degree at Tianjin University. His research interests include power system stability analysis, power system protection, and VSC-HVDC systems.

Guowei Liu is currently an Engineer in Shenzhen Power Supply Bureau Co., Ltd., Shenzhen, China. His current research interests include high-power electronics and power quality control.

Ming Lei is a Lecturer with the School of Electrical Engineering and Automation, Tianjin University, Tianjin, China. His research interests include circuit topology, control, and application of modular multilevel converters in HVDC power transmission and railway power system.

Chao Yang is currently a Professor with Sichuan Energy Internet Research Institution, Tsinghua University, Chengdu, China. His current research interests include clean energy power system optimization operation, and power electronic system analysis.

Chengshan Wang received the Ph.D. degree in electrical engineering from Tianjin University, Tianjin, China, in 1991. From 1994 to 1996, he was a Senior Academic Visitor with Cornell University, Ithaca, USA. From 2001 to 2002, he was a Visiting Professor with Carnegie Mellon University, Pittsburgh, USA. He is currently a Professor with the School of Electrical Engineering and Automation, Tianjin University, where he is also the Director of the Key Laboratory of Smart Grid of Ministry of Education. His current research interests include distribution system analysis and planning, distributed generation system and microgrid, and power system security analysis.